Structure
Article

Briefly Bound to Activate: Transient Binding of a Second Catalytic Magnesium Activates the Structure and Dynamics of CDK2 Kinase for Catalysis

Zhao Qin Bao,[1,2] Douglas M. Jacobsen,[1,2] and Matthew A. Young[1,*]
[1]Department of Biological Chemistry and the Bioinformatics Program, The University of Michigan Medical School, Ann Arbor, MI 48109, USA
[2]These authors contributed equally to this work
*Correspondence: youngmat@umich.edu
DOI 10.1016/j.str.2011.02.016

SUMMARY

We have determined high-resolution crystal structures of a CDK2/Cyclin A transition state complex bound to ADP, substrate peptide, and MgF_3^-. Compared to previous structures of active CDK2, the catalytic subunit of the kinase adopts a more closed conformation around the active site and now allows observation of a second Mg^{2+} ion in the active site. Coupled with a strong [Mg^{2+}] effect on in vitro kinase activity, the structures suggest that the transient binding of the second Mg^{2+} ion is necessary to achieve maximum rate enhancement of the chemical reaction, and Mg^{2+} concentration could represent an important regulator of CDK2 activity in vivo. Molecular dynamics simulations illustrate how the simultaneous binding of substrate peptide, ATP, and two Mg^{2+} ions is able to induce a more rigid and closed organization of the active site that functions to orient the phosphates, stabilize the buildup of negative charge, and shield the subsequently activated γ-phosphate from solvent.

INTRODUCTION

Protein kinases represent one of the fundamental components of cell-signaling pathways in all organisms. CDK2 is a mammalian Ser/Thr kinase that plays a critical role in controlling the progression from G1 to S phase of the cell cycle (Morgan, 1997). CDK2 is functionally homologous to the well-studied cdc28a *S. cerevisiae* protein. Consistent with its important role in influencing progression through the cell cycle, the activity of the enzyme is subject to many levels of regulation. Misregulation of CDK2 activity, for example through mutation, may contribute to the development of human cancers (Greenman et al., 2007; Malumbres and Barbacid, 2007; Milde-Langosch, et al., 2001), and CDK2 represents a potential therapeutic target (Malumbres and Barbacid, 2009). The isolated 34 kDa catalytic subunit of CDK2 exhibits relatively negligible catalytic activity, and the cellular concentration remains constant through the cell cycle. Maximum protein kinase activity is not obtained until the catalytic subunit is bound by an allosteric Cyclin protein (Radzio-Andzelm et al., 1995) and the catalytic domain has been phosphorylated on Thr-160, located within the kinase ''activation loop'' motif (Stevenson et al., 2002). The binding of Cyclin and the phosphorylation of Thr-160 have both been shown to stabilize large-scale conformational changes in the catalytic domain that function both to increase affinity for substrate (reduce K_M) as well as enhance the catalytic rate of the reaction (increase k_{cat}) (Brown et al., 1999b; Pavletich, 1999). In addition to allosterically upregulating catalytic activity upon binding to the catalytic domain, the Cyclins are also able to assist in the recruitment of specific protein substrates by binding to recruitment motifs. CDK2 is negatively regulated by the binding of a number of inhibitory proteins such as the $p21^{Cip}$ and $p27^{KIP}$ families, as well as by the phosphorylation of Tyr-15 and Thr-14 within the catalytic subunit. Multiple crystal structures are available for a number of the functional states of CDK2 (Pavletich, 1999).

Because they carry out very similar chemistries, it has been suggested that the majority of protein kinases may be subject to functional restrictions that require them to adopt very similar conformations when they are in their catalytically competent state. Hence, it could be the differences between their catalytically downregulated structures that might be responsible for much of their functional diversity (Huse and Kuriyan, 2002). Although there is growing evidence to support this hypothesis, direct structural and experimental data on active kinases caught in the act of catalysis have been difficult to obtain. Many enzymes catalyze similar reactions that liberate the γ-phosphate from a nucleotide triphosphate (NTP), but details such as the nature of the stabilizing protein side chains or the number of catalytic metals are not always conserved. Given the large number of protein kinases and the diverse signaling pathways they take part in, we cannot assume that they all operate using identical chemistries. For example, whereas many protein kinases are believed to require two divalent metal ions for optimum catalysis (Adams, 2001), it was recently established that at least one protein kinase, CASK, is only active in the complete absence of any divalent ions (Mukherjee et al., 2008). There is structural evidence that many kinases may only utilize a single divalent ion. The potential difference in the number of Mg^{2+} ions utilized by different kinases is especially important in the context of looking at the entire ensemble of over 500 protein kinases in the human genome (Manning et al., 2002) because identifying any differences in the details of how individual enzymes catalyze the reaction could provide important insight into the origins of functional and regulatory diversity among

kinases. This information could also contribute to our understanding of how activating mutations result in misregulation of specific kinases and could even be helpful in the rational design of specific protein kinase inhibitors. Kinase-specific differences in the function of the highly conserved "DFG" motif, which is essential for coordinating active site Mg^{2+} ions, are believed to be a critical determinant of the specificity profile of the clinically successful kinase inhibitor Gleevec as well as other DFG-out or "type-II" kinase inhibitors (Liu and Gray, 2006).

The most detailed model for the transition state (TS) conformation of a protein kinase is the AlF_3 TS mimic of protein kinase A (PKA) (Madhusudan et al., 2002). This 2.0 Å structure highlights a significant point of distinction between PKA and CDK2: all published structures of CDK2 bound to nucleotides identify at most a single Mg^{2+} ion in the active site, whereas the PKA TS structure clearly contains two catalytic Mg^{2+} ions that are in direct coordination with the reactive phosphates. Many NTP enzymes utilize a single metal ion, and a one Mg^{2+} (1Mg) mechanism for CDK2 is certainly reasonable. A structure of active CDK2 bound to nitrate (NO_3^-), a potential TS mimic, has been determined, showing a single Mg^{2+} ion in the active site (Cook et al., 2002), and a single Mg^{2+} mechanism for CDK2 has been proposed and shown to be energetically feasible via quantum mechanical simulations (De Vivo et al., 2007). Given the flexible nature of protein kinases, it is likely that a number of different protein conformations and ligand/activator states are sampled along the reaction cycle and that different structures may indeed represent different conformations within the same ensemble of transiently occupied states. Extensive studies of PKA support the notion that the role of Mg^{2+} ions at different stages of the catalytic cycle is dynamic and rather complex, with one of the two Mg^{2+} ions referred to as "essential" and the second as "inhibitory" (Shaffer and Adams, 1999b). Therefore, it is still uncertain whether CDK2 utilizes a single Mg^{2+} ion for the phosphoryl-transfer step and is truly different from the two Mg^{2+} (2Mg) mechanism observed in PKA or whether a 2Mg CDK2 state has just not yet been observed.

A related and also elusive question in the mechanism of protein kinases is the possible role that protein dynamics may play in both the catalytic mechanism as well as the regulation of catalytic activity. Structures of a number of protein kinases have revealed how flexible the catalytic domain can be, especially in facilitating the disassembly of the catalytically competent active site to adopt a downregulated state. It has been proposed that kinases, like other enzymes, may have evolved to channel or funnel specific protein motions in order to assist the reactants in sampling and progressing through the high-energy TS of the reaction (Henzler-Wildman et al., 2007; Kamerlin and Warshel, 2010), but this idea is difficult to prove (Kamerlin and Warshel, 2010; Li et al., 2002). Once again, the challenges associated with obtaining experimental and structural data on protein kinases at each step of the catalytic reaction have made it difficult to fully understand the functional roles of protein dynamics and its differences within the divergent protein kinases.

To better understand the detailed mechanism of the CDK2 kinase reaction, we have determined new crystal structures of an active Phosho-CDK2/Cyclin A complex bound to ADP, a substrate peptide, and MgF_3^-, a mimic for the γ-phosphate of ATP in the TS. We believe this complex provides an informative model of the structure of the enzyme during the phosphoryl-transfer step, one of the key rate-limiting steps of the reaction. We have carried out a series of molecular dynamics (MD) simulations to investigate the possible roles of protein dynamics in the catalytic mechanism of CDK2. Based on these results, we propose that the transient binding of a second activating Mg^{2+} ion to the active site of CDK2 helps facilitate the phosphoryl-transfer step by simultaneously closing down the active site by expelling water, electrostatically stabilizing the reactants, and reducing the conformational flexibility of the ATP.

RESULTS

Overall Structure of the Complex

The architecture of the phosphorylated P-Thr160 CDK2/Cyclin A complex (pCDK2/Cyclin A) bound to ADP/MgF_3^-/peptide is shown in Figure 1A. We have determined two independent but very similar structures of the complex, solved at slightly different pHs (Table 1). The overall conformation of the complex in the TS structures is similar to previously published structures of P-Thr160 CDK2 bound to Cyclin A, all crystallized in different buffer conditions and different space groups. The overall Cα rmsd to an ATP-γS bound CDK2/Cyclin A complex is 1.1 Å (Russo et al., 1996), and Cα rmsd to an AMPPNP/peptide CDK2/Cyclin A complex is 0.7 Å (Brown et al., 1999a).

A close-up view of the pCDK2/Cyclin A active site is shown in Figure 1B. Each structure contains two copies of the CDK2/Cyclin A complex, and we can clearly visualize the ADP, the 10-residue substrate peptide, and a trigonal-planar MgF_3^- ion positioned between the ADP β-phosphate and the Thr γ-O atom of the substrate peptide in each of them. A 2Fo-Fc electron density map of the reactants is shown in Figures 1D–1F, including distinct density for the 2Mg ions we observe. Each Mg^{2+} is in direct van der Waals contact with one of the fluorine atoms of the MgF_3^- phosphate mimic as well as five additional electronegative oxygen atoms at distances of 1.9–2.5 Å, described in more detail below.

MgF_3^- Transition State Mimic

A number of different chemical species have been employed along with an NDP to mimic the γ-phosphate TS in NTP reactions, including AlF_3, AlF_4^-, BeF_3, NO_3^-, and vanadate. Different species work best with different enzymes. Here, we use MgF_3^- as a TS mimic of the γ-phosphate of ATP. The titration of MgF_3^- into the CDK2 kinase reaction demonstrates that MgF_3^- is able to inhibit the CDK2 kinase reaction in vitro (see Figure S1 available online). The TS crystals were prepared by soaking apo crystals of the pCDK2/Cyclin A complex in buffer containing ADP, Mg^{2+}, NaF, and substrate peptide. To verify presence of MgF_3^- in the crystal, Figure 1A shows an Fo-Fc "average kicked" omit map calculated in PHENIX (Adams et al., 2010) after removing the MgF_3^- from the model. A series of studies have suggested that MgF_3^- can function as a superior TS mimic for certain phosphoryl-transfer enzymes because the −1 charge of MgF_3^- more closely resembles the true PO_3^- intermediate compared with neutral-charge species such as AlF_3 (Baxter et al., 2006, 2008; Graham et al., 2002). This hypothesis is supported by the observation that AlF_3 is sometimes converted to the square-planar AlF_4^- form when used as a TS mimic.

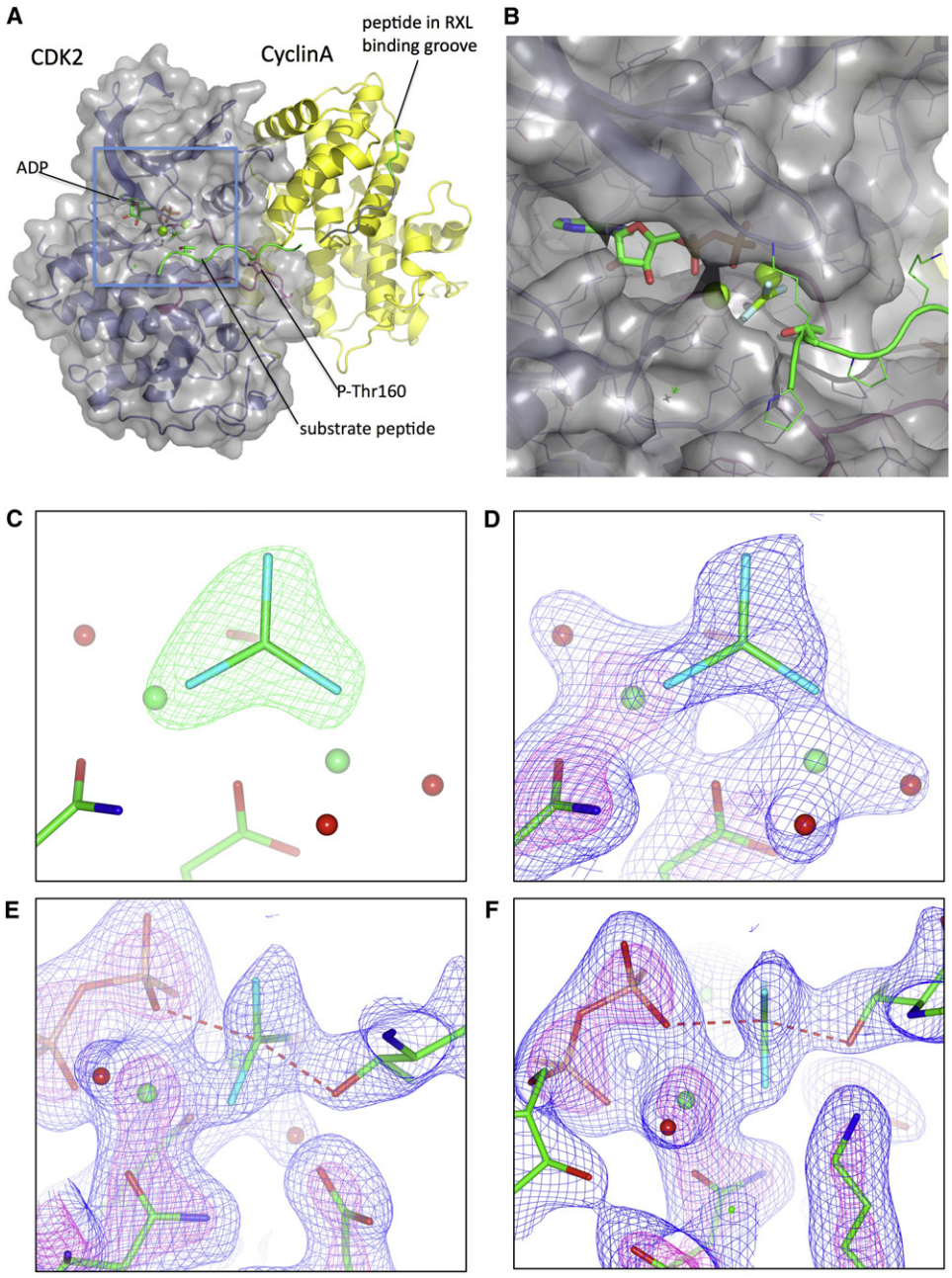

Figure 1. Structure of pCDK2/Cyclin A-ADP/MgF_3^-/Peptide Complex and Details of the Active Site

(A) Overview of the complex. Catalytic subunit is gray and Cyclin A is yellow.

(B) Close-up of the protein active site (region highlighted in A) showing the ADP, Mg ions, MgF_3^-, and the peptide substrate (green). The C-terminal region of a second copy of the substrate peptide (PKTPKK**AKKL**) was determined to have bound to the "RXL" substrate-binding groove on Cyclin A and is also shown in green. The N-terminal region of this peptide shown in gray is largely disordered and was modeled at zero occupancy.

(C) fo-fc difference map (5σ) from an averaged kicked omit map where the MgF_3^- was omitted from the model. (D–F) Three views of the 2fo-fc electron density (blue, 1.25σ; magenta, 3.5σ) at the active site. Red spheres are waters and green spheres are Mg^{2+}.

See also Figure S1.

The trigonal-planar MgF_3^- in the CDK2 TS structures is coordinated by a number of positively charged protein atoms as well as metal ions, suggesting that reproducing the −1 charge of the true PO_3^- metaphosphate anion intermediate (Westheimer, 1987) is important.

Glycine-Rich (Gly-rich) Loop

The conformation of the Gly-rich loop (residues 10–18) that functions somewhat like a lid on top of the ATP phosphates is quite different from what has been observed in all previously published structures of the pCDK2/Cyclin A complex. As shown in Figure 2,

Table 1. Data Collection and Refinement Statistics

	pCDK2/Cyclin A/ADP/MgF_3^-/Peptide (pH 8.0)	pCDK2/Cyclin A/ADP/MgF_3^-/Peptide (pH 8.25)
Data Collection		
Space group	$P2_1$	$P2_1$
Cell dimensions		
a, *b*, *c* (Å)	*a* = 70.69, *b* = 163.91, *c* = 73.28	*a* = 71.03, *b* = 163.45, *c* = 73.39
α, β, γ (°)	α = 90.0, β = 107.38, γ = 90.0	α = 90.0, β = 107.08, γ = 90.0
Resolution (Å)	2.17 (2.29–2.17)[a]	1.91 (2.01–1.91)[a]
R_{sym}	13.2 (112)	14.0 (114)
$I/\sigma I$	7.4 (1.5)	8.6 (1.5)
Completeness (%)	100 (100)	100 (100)
Redundancy	3.9 (3.8)	7.6 (7.5)
Refinement		
Resolution (Å)	37.8–2.17	39.75–1.91
Number of reflections	323,456 (83,902 unique)	935,485 (123,328 unique)
R_{work}/R_{free}	17.38%/20.71%	19.02%/21.42%
Number of atoms	10,089	10,041
Protein	9,476	9,348
Ligand/ion	33	33
Water	613	684
B factors		
Protein	54	42
Ligand/ion	66	46
Water	59	47
Rmsd		
Bond lengths (Å)	0.012	0.008
Bond angles (°)	1.3	1.1

Values in parentheses are for highest-resolution shell.
[a] Data were collected from a single crystal.

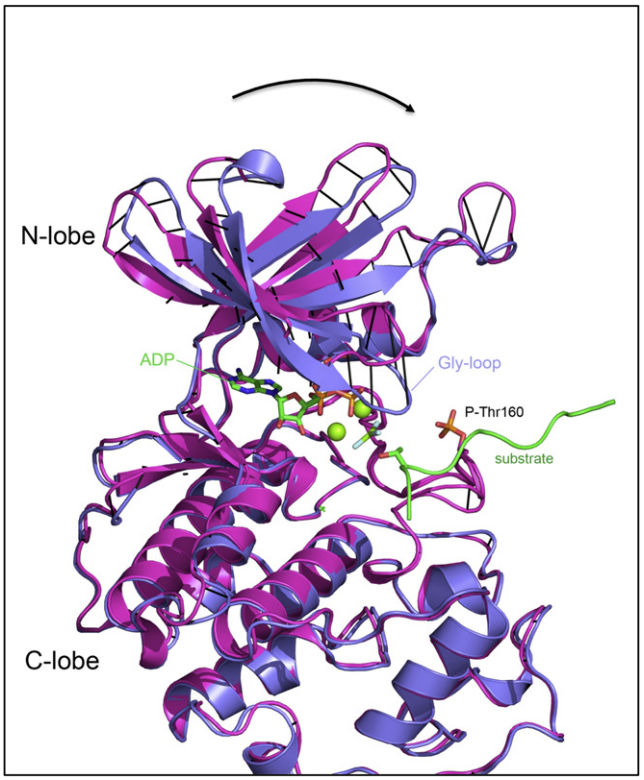

Figure 2. Motion of the N-Lobe Induced upon Binding of Peptide Substrate and the Second Mg^{2+} Ion

Magenta is 1JST.pdb, the pCDK2/Cyclin A complex bound to ATP and 1 Mn^{2+} ion. Blue is the TS structure of pCDK2/Cyclin A bound to ADP/MgF_3^-/2×Mg^{2+}/peptide substrate. The structures were aligned on α-Carbons (C_α) of the whole complex using PyMOL (DeLano, 2010 [Schrödinger, LLC, Cambridge, MA, USA]) with black lines drawn to indicate equivalent C_α atom positions.

the N-lobe of the kinase is rotated clockwise in the direction of the nucleotide phosphates relative to 1JST.pdb, a structure of ATP γ-S bound pCDK2/Cyclin A with a single Mn^{2+} ion, such that the TS conformation significantly reduces the volume of the nucleotide-binding pocket that sandwiches the phosphates. Although there is considerable variation in the N-lobe position between the two conformations, Lys-33, which interacts with both an ATP α-phosphate oxygen and Glu-51 in α helix C, is nearly structurally invariant between the two conformations and appears almost to function as a fixed pivot point for the N-lobe rotation and closure.

We compare the conformation of the CDK2 Gly-rich loop TS structure with four published structures of pCDK2/Cyclin A bound to ATP analogs in Figure 3. The range of Gly-rich loop conformations illustrates the flexibility of this substructure. The conformations of the nucleotide phosphates in these structures, especially the β- and γ-phosphates, appear to mirror this flexibility. Despite the range of conformations observed for the ATP phosphates and the local flexibility of the Gly-rich loop, the positioning of the flexible Gly-rich loop in our TS structure (indicated in gray in Figure 3B) is a notable outlier. The conformation of the Gly-rich loop in the TS has closed down in such a way that the backbone amides make direct interactions with both the ADP β-phosphate and the MgF_3^- γ-phosphate mimic. The Gly-rich loop region of the protein is far from any crystallographic neighbors in the TS structure, so it is not likely to be a consequence of crystal packing.

This closed conformation of the TS Gly-rich loop is similar to the one observed for the inactive state of the CDK2 catalytic domain (1HCK.pdb) (Schulze-Gahmen et al., 1996). Although the conformation of the unphosphorylated activation loop in the inactive CDK2 monomer inhibits substrate peptide from binding via steric hindrance, we believe that the similar Gly-rich loop conformation attests to the thermodynamic stability of the closed conformation of the Gly-rich loop for CDK2.

The structure of the CDK2 TS Gly-rich loop is also strikingly similar to the structure of the TS mimic structure of PKA bound to ADP/AlF_3 and a high-affinity PKI-derived substrate

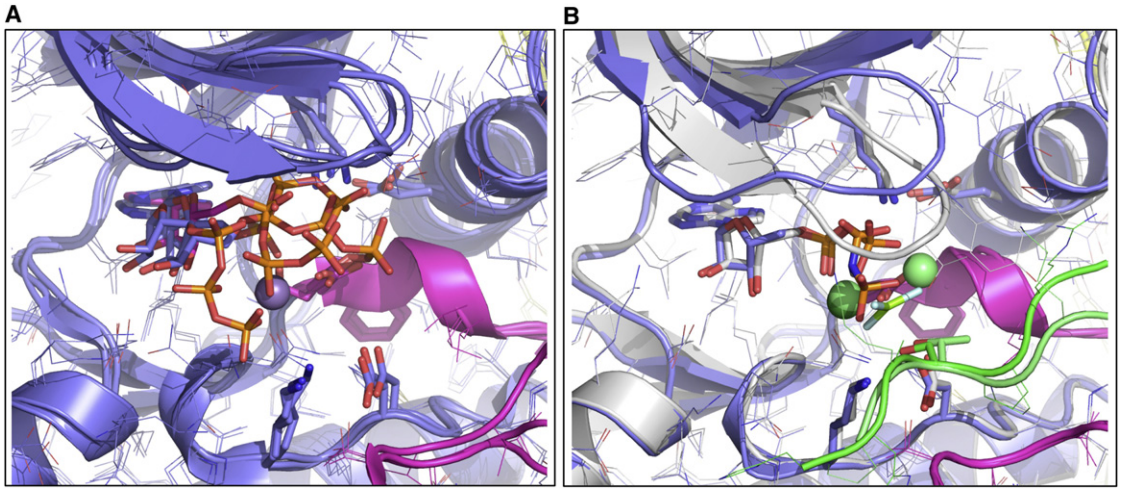

Figure 3. A Comparison of the Active Site Region of CDK2/Cyclin A Bound to ATP Analogs and CDK2/Cyclin A with the TS Complex
(A) A superimposition of three independent crystal structures of the CDK2/Cyclin complex showing the different conformations of the nucleotide and Gly-rich loop (pdb entries: 1fin, 1jst, 2hcc). Residues in the kinase activation loop (145–168) are colored magenta.
(B) Superposition of 1QMZ.pdb, pCDK2/Cyclin A bound to AMPPNP/1Mg ion/substrate peptide (blue), with the TS structure (gray).

peptide(1L3R.pdb, Figure 4). Although the TS active site conformations are very similar, CDK2 is different from PKA because it appears to undergo both structural changes and an overall ordering of the active site when transitioning from the ATP-bound state to the TS conformation, whereas PKA was described to undergo only very slight structural changes (Madhusudan et al., 2002). However, it should be noted that recent results and discussion point to the possibility that the PKA Gly-rich loop might also behave in a more dynamic way and undergo open to closed motions similar to what we see in CDK2 (Masterson et al., 2010) when not interacting with high-affinity peptide inhibitors (Zimmermann et al., 2008).

Two Magnesium Ions

To the best of our knowledge, these are the first pCDK2/Cyclin A crystal structures grown in the presence of Mg^{2+} because Mg^{2+} was observed to inhibit the growth of other CDK2/Cyclin A crystal forms (Jeffrey et al., 1995). The TS crystals were grown in the presence of 20 mM Mg^{2+} and were then transferred and soaked in a solution containing a more physiologically relevant 10 mM $MgCl_2$ prior to mounting. This might have resulted in our ability to identify 2Mg ions in the TS structure, which was not previously reported for other CDK2 structures. A series of views of the active site of the TS structure including the 2Mg ions are shown in Figure 5. The ions have been labeled MgI

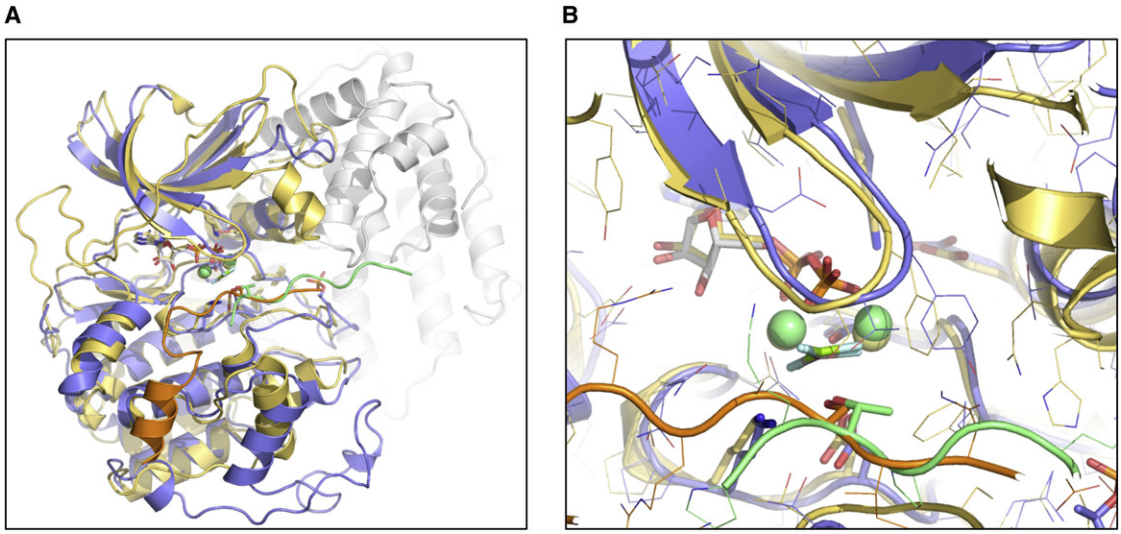

Figure 4. Comparison of the CDK2 TS Complex with PKA
(A) Superimposition of the TS mimic complexes of CDK2 and PKA (1l3r.pdb). CDK2 is blue/green, Cyclin A is gray, and PKA is gold/orange.
(B) Close-up of the active sites.

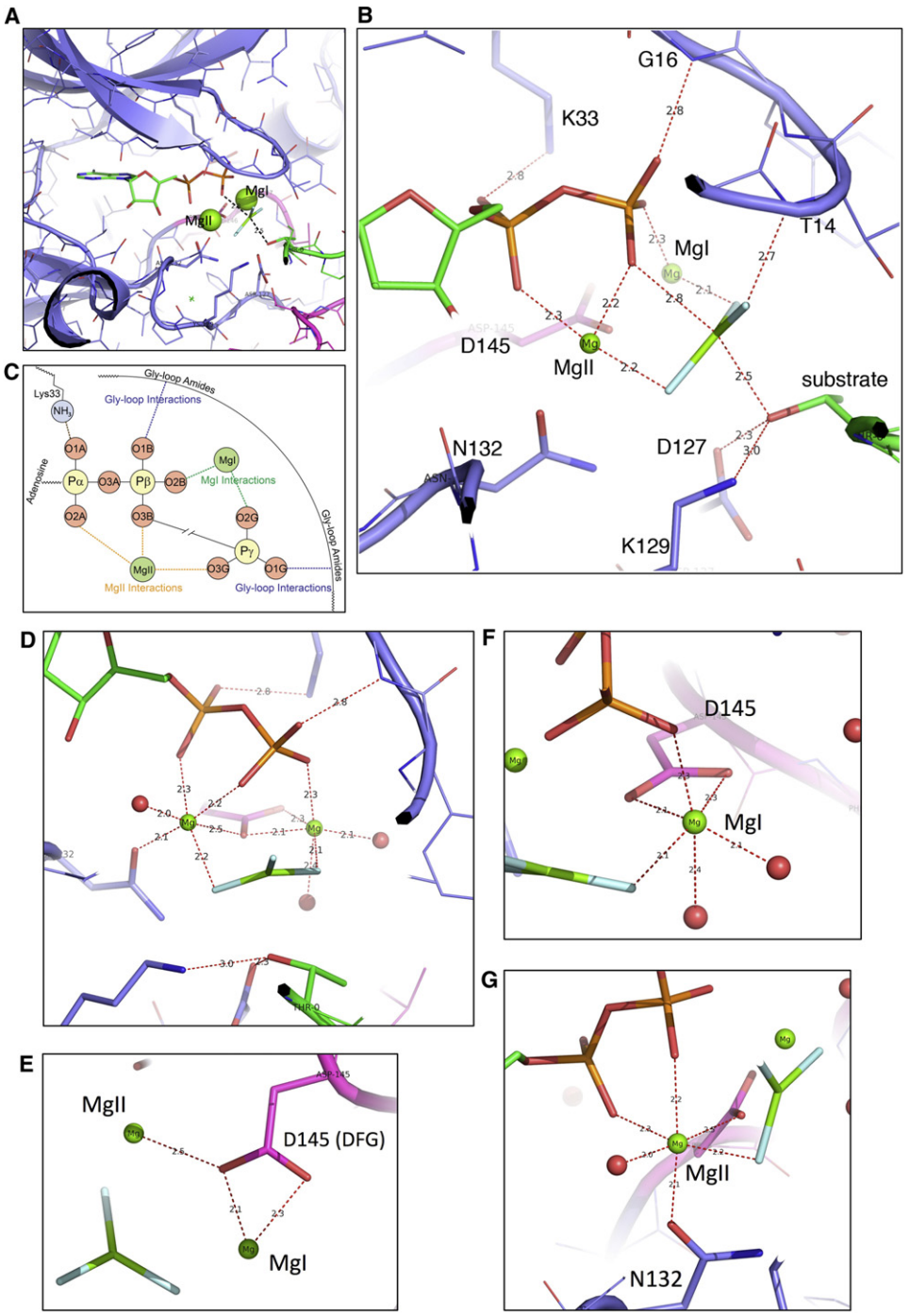

Figure 5. Coordination of the Reactants and Mg^{2+} Activators in the CDK2 Active Site (MgI has not been seen in previous CDK2 nucleotide structures)

(A) Overview showing MgI and MgII (green) at 50% VdW contact radius.

(B) Close-up highlighting the phosphate and substrate Thr interactions: α-phosphate, Lys33,MgII; β-phosphate, Gly16-NH,MgI,MgII; γ-phosphate(MgF_3^-),MgI,MgII,Thr14-NH; and substrate Thr, Asp127,Lys129. Amides from the Gly-rich loop contact both the β- and γ-phosphates. Asp127 and Lys129 participate in hydrogen bonds with the reactive substrate Thr.

(C) Schematic of ATP phosphate interactions.

(D) Coordination environment of the two Mg ions.

(E) Coordination of Asp145 in the DFG motif.

(F) MgI is coordinated by both Asp145 (DFG) oxygens, two waters, the β-phosphate, and the γ-phosphate mimic.

(G) MgII is coordinated by Asn132, the α- and β-phosphates, a water, and the γ-phosphate mimic.

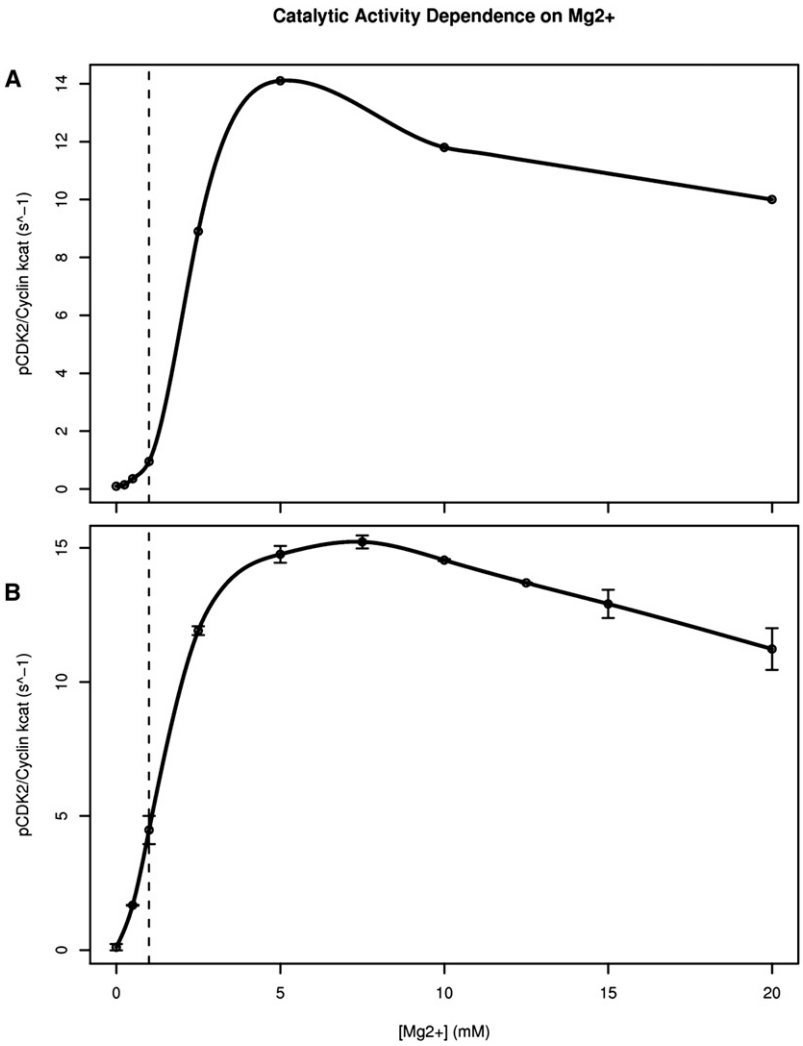

Figure 6. Mg^{2+} Dependence of the Reaction

Activity of the pCDK2/Cyclin A complex as a function of Mg^{2+} concentration. The dashed line indicates 1 mM $[Mg^{2+}]$ where the 800 μM ATP is expected to be saturated with one bound Mg^{2+}. (A) Assay using γ-P^{32}-labeled ATP and peptide substrate. (B) Coupled kinase assay using histone H1 substrate. Both assays were performed with saturating substrate concentrations. Error bars indicate standard error over all replicates.

and MgII, consistent with the nomenclature used in other protein kinases (Adams, 2001). Although MgI has been described as the "essential" catalytic Mg^{2+} in PKA and MgII as "inhibitory" (Cook et al., 1982; Shaffer and Adams, 1999b), MgII is the only Mg^{2+} that has been observed in previously published structures of pCDK2/Cyclin A, and the MgI site has always been unoccupied. In the CDK2 TS structure, MgII is observed to be in a classic hexa-coordinate octahedral geometry with distances between Mg^{2+} and ligands ranging between 1.8 and 2.5 Å (Figures 5D and 5G). It is coordinated by a single water molecule, the ADP α- and β-phosphate oxygen, one of the MgF_3^- fluorine atoms, Asn132 δ−O, and one oxygen from Asp145 of the conserved kinase DFG motif. The second Mg^{2+} ion we observe (Figures 5D and 5F) is positioned in precisely the same position as MgI in the PKA TS. Unlike MgII, MgI is not in an ideal octahedral Mg^{2+} coordination geometry. This is largely due to the fact that it is positioned at the bisector of the two Asp145 (of the DFG motif) oxygens. The 2.1 and 2.3 Å distances to each of these oxygens result in a roughly 60° angle (Figure 5E), rather than the 90° angle found in the ideal octahedral coordination geometry. The other coordinating groups include two waters (2.2 and 2.5 Å), an ADP β-phosphate oxygen (1.9 Å), and one MgF_3^- fluorine (2.2 Å). Although the geometry is not a perfect octahedron, this "bidentate" Mg^{2+} coordination has been determined to be the most stable conformation for Asp or Glu:Mg interactions in certain cases (Dudev and Lim, 2004), and we believe the distances to the coordinating oxygens are too short for this to be either a water or a monovalent Na^+ ion. It is possible that the imperfect geometry could result in MgI being less thermodynamically stable compared to MgII, which could partially explain why MgI has not been observed in other pCDK2/Cyclin A structures. The 2Mg TS structure also places a slight strain on the backbone of the DFG motif residues.

Mg^{2+} Dependence of the Reaction

To evaluate the functional relevance of the 2Mg ions, we have carried out in vitro kinase assays to measure the reaction velocity as a function of Mg^{2+} concentration (Figure 6). The nonhyperbolic shape of the curve indicates a potentially complex behavior. Although activity is barely detectable at less than 1–2 mM $[Mg^{2+}]_{total}$, the reaction velocity begins to be slightly inhibited by $[Mg^{2+}]$ greater than about 5–7 mM. This type of curve has been observed for other kinases (Liu et al., 2010; Sun and Budde, 1997; Waas and Dalby, 2003), and a number of models have been proposed to explain the behavior. All models invoke a second essential activating Mg^{2+} to explain the sharp stimulatory $[Mg^{2+}]$ effect at 0–5 mM $[Mg^{2+}]_{total}$. Because the stability constant of the first Mg^{2+} to ATP equates to a K_D in the low micromolar range (O'Sullivan and Smithers, 1979), the 800 μM ATP^{4-} in this reaction should become saturated with a single Mg^{2+} at concentrations only about 50–100 μM higher than what is needed for 1:1 stoichiometry, i.e., at less than 1 mM total Mg^{2+}. So, consistent with earlier crystal structures, ATP×1Mg is the species that would be available to bind to the protein at 1 mM Mg^{2+}. The fact that we observe almost no activity at this concentration of Mg^{2+} indicates that an additional Mg^{2+} ion is needed at some step of the reaction. Details of these models will be discussed in the next section.

Positioning and Activation/Stabilization of the Nucleophile

Two different basic reaction mechanisms have been proposed for the majority of protein kinases (Adams, 2001; Cook et al., 2002; De Vivo et al., 2007). They differ primarily in the mechanism

of the substrate OH group activation. In the first reaction scheme, the substrate OH (a threonine side chain in this structure) is deprotonated, most likely by a residue acting as a general base, to activate and stabilize the electronegative substrate oxygen that acts as a nucleophile to attack the closely positioned γ-phosphate. The primary difference in the second reaction scheme, sometimes referred to as "substrate catalysis," is that the phosphate transfer is initiated via a simultaneous transfer of the substrate OH proton to one of the ATP γ-phosphate oxygens rather than a protein side chain. Therefore, the key difference is in the mechanism of deprotonation. The present structure places the Thr oxygen 2.3 Å from Asp127 and 2.6 Å from the closest MgF_3^- fluorine, thus within a H-bond distance from either of these potential proton acceptors (Figure 5). To distinguish between the two schemes, it may be important to note that Lys129 is positioned roughly 3.2 Å from the phosphate-mimic F closest to the substrate Thr and 3.0 Å from the substrate Thr oxygen. This orientation, along with the additional cation:MgF_3^- interactions described below, would significantly decrease the likelihood that a γ-phosphate oxygen could accept a proton from the Thr-OH in its current environment. However, it would allow Lys129 to help stabilize the buildup of charge on the (unprotonated) γ-phosphate and ensure its correct alignment with the Thr-O^- as it is being transferred. If this is what is occurring, Asp127 is optimally positioned to function either as a general base to enhance the substrate's reactivity as a nucleophile, or to function as a proton trap or shuttle (Valiev et al., 2003) functioning to align and accept the proton from the substrate Thr via the first reaction scheme (Zhou and Adams, 1997).

In both schemes the destabilization of the dissociating β-γ-phosphate bond can be accelerated by the action of one or two divalent metal ions, possibly assisted and/or substituted by additional cationic groups, that stabilize the buildup of negative charge on the β- and γ-phosphates via direct interaction with the phosphate oxygens. If the γ-phosphate is subject to nucleophilic attack while it is still closely associated with the β-phosphate and proceeds through a penta-coordinated intermediate, the reaction is classified as "associative." Alternatively, if the γ-phosphate largely breaks the connection to the β-phosphate and forms a trigonal-planar anionic intermediate before nucleophilic attack, it is classified as a dissociative reaction. These are two extremes of the reaction intermediate, and most phosphoryl-transfer reactions probably exist somewhere in between (Mildvan, 1997).

The geometry of the CDK2 TS structure more closely resembles a dissociative TS, but it is not 100% dissociative. In monomer A the distances of the γ-phosphate mimic to both the ADP leaving group and Thr nucleophile are 2.75 and 2.5 Å. In the two extreme reaction mechanisms, the ideal O-P TS distance in a 100% associative reaction is 1.73 Å, whereas the fully dissociative O-P distance is 3.3 Å (Mildvan, 1997). Once formed, the final O-P phosphate covalent bond is roughly 1.6 Å. Based on the total O-P-O distances alone, the TS is roughly 57% dissociative: 100% associative = 3.46 Å < TS crystal = 5.25 Å < 100% dissociative = 6.6 Å. Although we cannot rule it out from the current structure, the generation of a purely penta-coordinated associative intermediate would require significant additional motion in the active site to simultaneously bring the ADP and peptide Thr oxygen close enough to one another to form the associative penta-coordinated γ-phosphate bridge. What is also evident from this structure is that further protein and reactant motion is not necessarily required for the phosphoryl transfer to occur because the total $O_{leaving}$-P_γ-$O_{nucleophile}$ distance is already considerably less than what is observed in a purely dissociative reaction.

Protein Dynamics of CDK2

In order to clarify the role of Mg^{2+} ions in the CDK2 active site and better understand the structural consequences of having either one or two Mg^{2+} ions present, we have carried out a series of explicit-solvent MD simulations of both the TS complex and the ATP-bound complex coordinated to either one or two Mg^{2+} ions.

TS-mimic simulations were carried out with a deprotonated Thr on the substrate peptide (the proton was transferred to Asp127) because this state is more stable in the simulations and may be what is present in the crystal. A 50 ns simulation of the ADP/MgF_3^-/2Mg^{2+}/peptide complex demonstrates the stability of the crystallized conformation. The backbone atom rmsd of the simulation structures fluctuates at 1.70 ± 0.17 Å from the TS crystal structure, and the rmsd of the average atomic structure computed over the entire MD trajectory relative to the crystal structure is 0.98 Å. As shown in the top time series panel in Figure 7, the Gly-rich loop remains in the closed conformation, and the Gly-rich loop amides maintain one or more direct contacts with the β-phosphate and/or MgF_3^- throughout the entire 50 ns trajectory.

We have found that the substrate peptide can be quite flexible and somewhat weakly bound in simulations of the ATP-bound complex, and to minimize simulation-sampling limitations, here, we report results from ATP simulations carried out without a substrate peptide. The instability of the substrate peptide in the simulations is consistent with the somewhat weak apparent affinity of this peptide (K_M = 120 μM at 150 mM KCl) (Figure S2). Full-length protein substrates are typically much better substrates for CDK2, due to stabilizing interactions located outside of the active site, e.g., the substrate-binding groove found in the Cyclin A subunit (Brown et al., 1999a).

Gly-Rich Loop Conformations

Figures 7D and 7E show superimpositions of snapshots at 1ns intervals from one of the two Mg simulations and one of the 1Mg ATP simulations. These simulations were both started from the same AMPPNP×1Mg/peptide structure (1QMZ.pdb), but the second Mg^{2+} ion was modeled in the MgI site for the 2Mg simulation. Data are also shown from an additional 1Mg simulation started from a different ATP structure (1JST.pdb). Although both the 2Mg and 1Mg simulations are very stable overall (backbone rmsd = 2.0 and 1.6 Å relative to the 1QMZ.pdb starting structure, respectively), we find that the presence of the second Mg^{2+} ion results in two notable changes to the CDK2 active site: (1) a spontaneous transition to the closed conformation of the Gly-rich loop seen in the TS structure, and (2) considerably less motion of the ATP phosphates. Considerable motion is observed in the Gly-rich loop in the beginning of all three simulations, but roughly 18 ns into the 2Mg simulation, the Gly-rich loop closes down and remains in that conformation for the duration of the 50 ns trajectory. Once closed, the Gly-rich loop backbone amides make direct contacts with both the

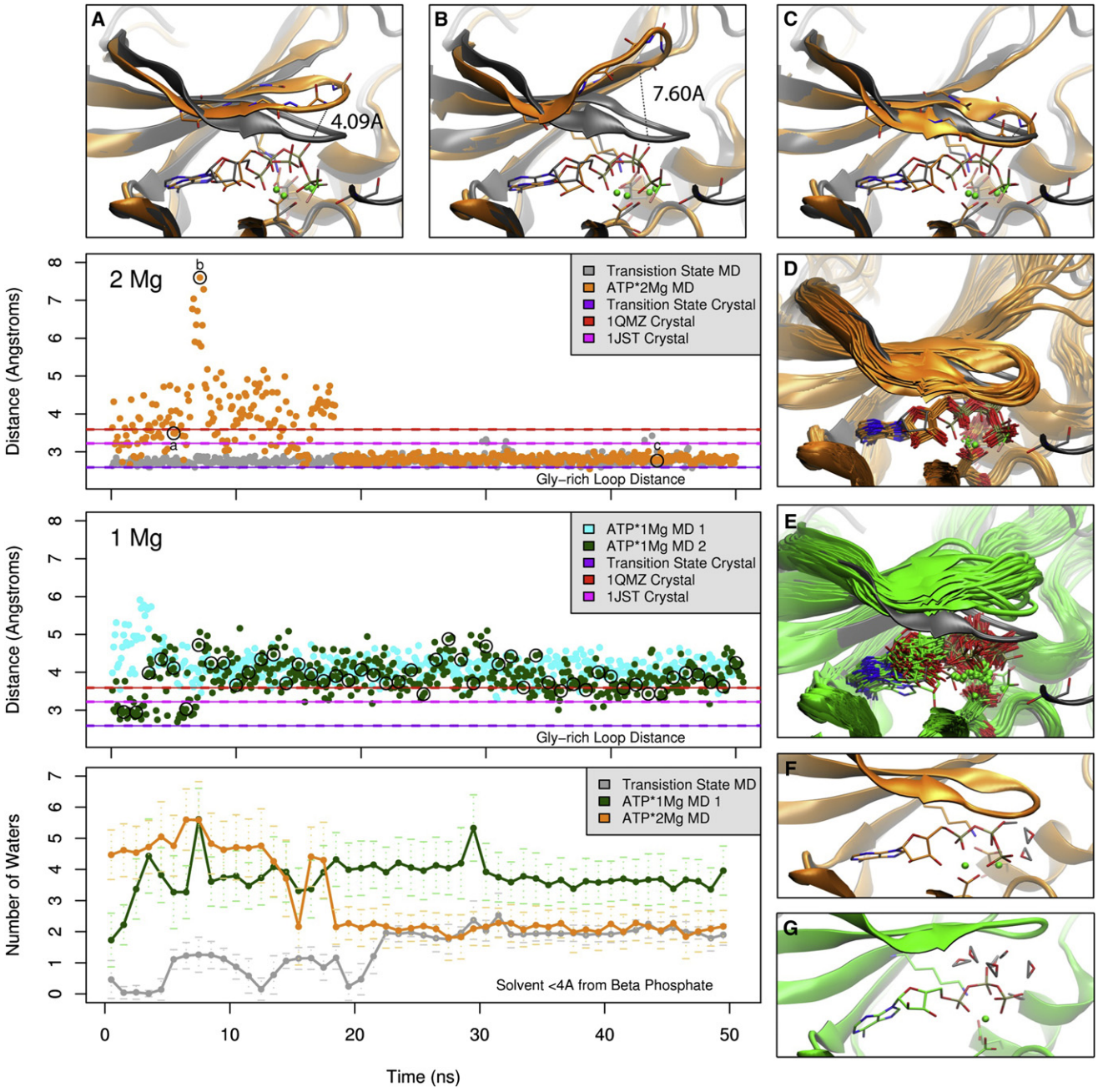

Figure 7. Structures and Analysis from Four MD Simulations of the pCDK2/Cyclin A Complex

The simulations predict that the binding of the second Mg ion in the active site (MgI position) stabilizes the down conformation of the Gly-rich loop, expels waters from around the nucleotide phosphates, and reduces the conformational flexibility of the phosphates.

(A–C) Three snapshots (orange) from a simulation of pCDK2/Cyclin A bound to ATP and 2Mg ions beginning from1QMZ.pdb (pCDK2/Cyclin A/AMPPNP/1Mg/peptide). The crystal structure of the TS is superimposed in gray. A second Mg was placed in the MgI site at the start of the simulation. The Gly-rich loop converts to the closed conformation after ~18 ns.

(D) A superposition of 1 ns interval snapshots from the last 30 ns of the trajectory, after the Gly-rich loop has adopted the closed conformation.

(E) One nanosecond interval snapshots from a 50 ns simulation also starting from 1QMZ.pdb but with only 1Mg bound in the active site (MgII position). The top and middle time series graphs quantify the Gly-rich loop proximity to the ATP phosphates by measuring the distance from the ATP or ADP β-phosphate to the closest amide group in the Gly-rich loop. The origins of the structures shown in (A)–(C) and (E) are indicated with circles. The top graph shows simulations of the TS mimic (gray) and the 2Mg×ATP pCDK2/Cyclin A complex. The middle graph illustrates two simulations of pCDK2/Cyclin A bound to 1Mg and ATP. The corresponding distances measured in three crystal structures are indicated by horizontal lines. The bottom graph is a measurement of the number of waters less than 4 Å away from the ATP/ADP β-phosphate during the indicated trajectories (1 ns window average with 1 standard deviation).

(F and G) Snapshots from the 2Mg (F) and 1Mg (G) trajectories showing the waters less than 4 Å away from the ATP phosphates.

See also Figure S2.

ATP β- and γ-phosphates (Figure 7C). This closed conformation (shown in Figures 7C and 7D) is virtually identical to the conformation observed in the TS crystal structure (superimposed in gray).

The closed conformation of the Gly-rich loop is only sampled once a layer of water molecules located between the Gly-rich loop and the ATP phosphates has been expelled. The number of water molecules found less than 4 Å away from the β-phosphate is shown in the bottom time series plot in Figure 7. The closing down of the Gly-rich loop, seen at ~18 ns in the top time series plot, is concurrent with the discreet drop in the number of waters directly contacting the phosphates indicated in the bottom panel. Once the layer of phosphate-solvating waters has been expelled, the number of waters interacting with the phosphates remains exactly the same as is observed for the TS-mimic simulation. Thus, the analysis in the time series panels in Figure 7 indicates that direct ATP phosphate:water interactions are replaced by direct interactions with Gly-rich loop backbone amides when the Gly-rich loop adopts the closed TS-like conformation.

We have also observed that the Gly-rich loop spontaneously transitions in the opposite direction, from closed to open, when simulations are started with the closed (TS) conformation but with only a single Mg^{2+} bound to the ATP. The simulations as a whole clearly support a model where the Gly-rich loop exchanges between closed and open conformations and that the population of the open-closed equilibrium is strongly influenced by the binding of the second Mg^{2+} at the MgI site. All of these simulations have been repeated after randomizing ion positions within the solvent. In total, four out of five 2Mg simulations started from the open Gly-rich loop conformation transitioned to a closed conformation within 50 ns, and three out of five 1Mg simulations started from the closed Gly-rich loop conformation transitioned to an open conformation during the same time period. This Gly-rich loop equilibrium is also supported by the TS crystal structures. We have been able to build one of the four CDK2 TS Gly-rich loops reported here into two 50% occupancy closed and open conformations, and the occupancy of the MgI site in this subunit is somewhat less well defined.

Reduced Motion in the Active Site

In addition to influencing the closing of the Gly-rich loop, the simulations also indicate that the binding of the second Mg^{2+} ion notably reduces the magnitude of nanosecond timescale fluctuations for the ATP phosphates, Gly-rich loop, and the active site region of the protein. This is evident both in the structural superimpositions shown in Figures 7D and 7E and in the analysis shown in Figures 8A–8C, depicting backbone protein flexibility by drawing ellipsoids describing the extents of 50% positional occupancy of the protein Cα, nucleotide, and Mg^{2+} ions over the 20–50 ns time period of each simulation. The results show that there is a hierarchy of nanosecond timescale flexibility at the protein active site that is correlated with both substrate and activator Mg^{2+} binding. The most flexible state is the ATP×1Mg complex, followed by the ATP×2Mg complex, and the least flexible is the 2Mg ADP/TS/peptide complex.

The multiple ATP phosphate conformations the CDK2 active site is able to accommodate (Figures 3A and 3B) probably reflect an equilibrium of states that exists prior to the phosphoryl-transfer event. Although we do not observe interconversion between the precise crystal structure conformations within the current simulation time periods, we suggest that the differences in the nanosecond timescale dynamics between the ATP×1Mg and ATP×2Mg states are reporting on the relative flexibilities of these two states. By replacing diffuse water interactions with explicit Gly-rich loop amide and direct Mg^{2+} interactions, the ATP phosphates become more tightly integrated into an extensive scaffold of ionic interactions within the protein active site. What follows is that the binding of the second Mg^{2+} ion not only reduces the magnitude of the nanosecond timescale fluctuations of the ATP, but the additional ionic interactions it enables may also limit the permitted conformations of the ATP phosphates.

Taken together, this model and the available structural data suggest that the binding of the second activating Mg ion must be an ordered, possibly sequential, event that results in numerous changes to the active site that contribute to phosphoryl transfer when it occurs after ATP×1Mg binding during the catalytic cycle. In addition to directly coordinating the ATP β-phosphate, the binding of the second (MgI) ion results in the ATP simultaneously becoming more ordered, more shielded from solvent, and participating in additional ionic interactions with the protein. Simulations of the ATP×1Mg state containing only a single Mg at the MgII site suggest that the MgI site would certainly be accessible to ions from outside the protein because we consistently observe transient localization of monovalent Na^{+} ions from the simulation bulk solvent into the vacant electronegative MgI site. Free Mg^{2+} ions were not present in the simulation bulk solvent. Simulations starting with a single Mg at the MgI site are less stable and, thus, consistent with the crystallographic evidence that the MgII site is the first to become populated when ATP×1Mg binds.

Catalytic Mechanism

The CDK2 TS structure illustrates how CDK2 achieves two general mechanisms that enzymes can employ to accelerate chemical reactions: (1) correctly positioning the reactants in the optimum orientation, and (2) electrostatically stabilizing the high-energy TS and/or product leaving groups. The structural and dynamic changes of the CDK TS relative to reactant complexes support a model where the enzyme only optimally performs both of these rate-enhancing mechanisms once all the necessary ligands are bound in the active site. Notably, if either the second activating Mg^{2+} ion (MgI) or the peptide substrate is missing from the active site, the Gly-rich loop is predominantly in the up conformation, and the position of the β- and γ-phosphates is more delocalized and flexible. As all of the reactants bind, the complex network of ionic interactions is completed, the active site becomes less flexible, and the restricted flexibility may force the phosphates to converge upon the TS geometry.

Positioning the Phosphates and Holding Them Still

Further evidence that optimal phosphate alignment appears to be correlated to the binding of the second Mg^{2+} ion is the observation that each of the 1Mg crystal structures and MD simulations lacks one or more of the direct phosphate interactions that are observed in the TS structure shown in Figures 5B and 5C. This is in addition to missing the direct MgI:phosphate interactions. In particular the β-phosphate is held in place by direct interactions with MgII:O3B, MgI:O2B, and Gly16(NH):O1B, and

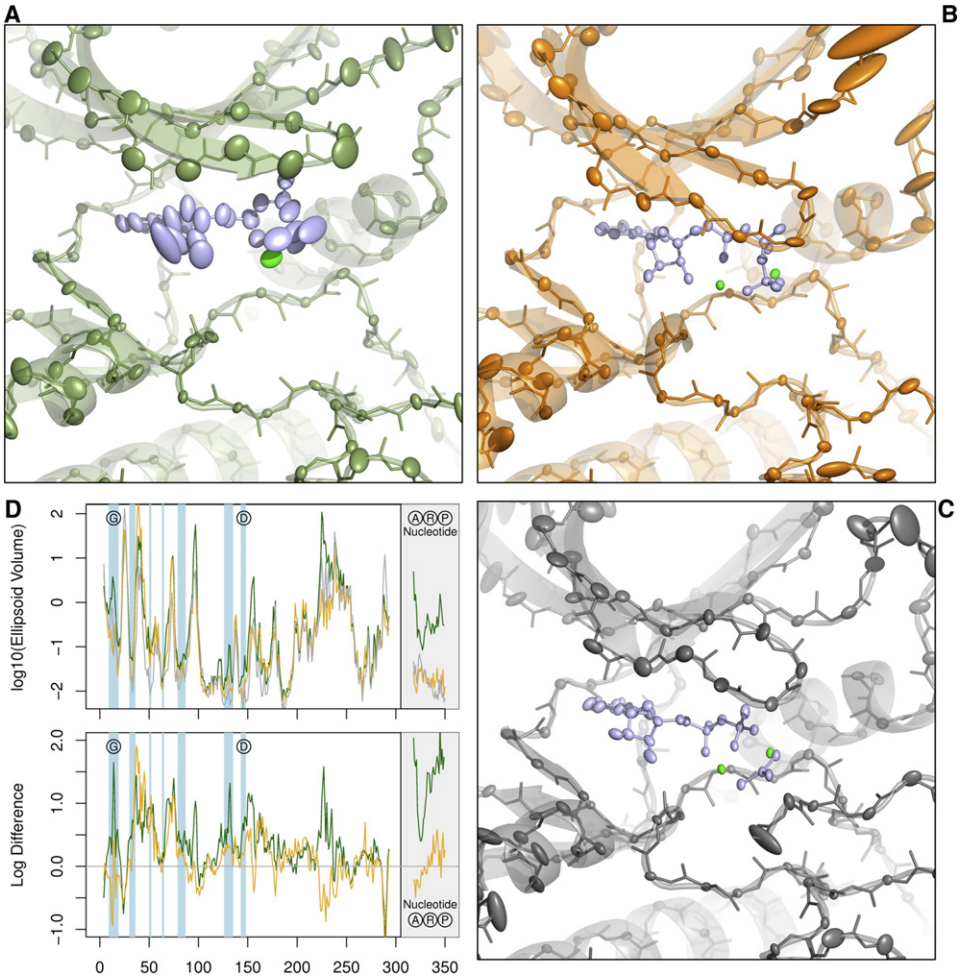

Figure 8. Extent of Protein Backbone Fluctuations in Three MD Trajectories

Anisotropic thermal ellipsoids are displayed to encompass 50% atomic positional probabilities for the Cα atoms, computed relative to the average atom positions over the 20–50 ns time period of each simulation. Simulations are the same as in Figure 7.

(A) pCDK2/Cyclin A with ATP and 1Mg.

(B) pCDK2/Cyclin A with ATP and 2Mg.

(C) pCDK2/Cyclin A/ADP/2Mg/MgF_3^-/substrate peptide.

(D) The top graph indicates the extent of fluctuation for each residue by plotting the $\log_{10}$ of the 50% probability Cα ellipsoid volumes. The bottom plot shows the difference between the fluctuations ($\log_{10}$ ellipsoid volumes) in the TS simulation and the 1Mg (green) and 2Mg (yellow) simulations. Shaded regions indicate residues within 5.0 Å of the nucleotide. G, the Gly-rich loop; D, DFG region; A, R, P, adenosine, ribose, and phosphate atoms in the ATP.

the MD simulations find that not a single one of these three interactions is maintained in the 1Mg-bound state. The γ-phosphate mimic is held in place by interactions with MgII:O3G, MgI:O2G, and Thr14(NH):O1G. The only one of these γ-phosphate interactions observed in the 1Mg state is MgII:O2G. Although the MD finds that the position of the γ-phosphate may not be as sensitive to the loss of the stabilizing interactions in the 1Mg state as the β-phosphate is, the orientation of the β-γ-phosphate linkage that is cleaved in the reaction is still nonoptimal in the 1Mg state as a result of the flexible β-phosphate position.

In addition to being affected by the binding of MgI, the conformation of the β-phosphate may also be sensitive to the presence of substrate peptide. In the simulation of CDK2 bound to ATP×2Mg, but without peptide, both MgI and the Gly-rich loop amides make stabilizing interactions with O1B and O2B of the β-phosphate, but the MgII:O3B interaction that was present in the beginning of these simulations is not preserved. O3B is the β-γ bridging oxygen that is dissociated from the γ-phosphate during the reaction. The MgII:O3B interaction is observed in 1QMZ.pdb, a structure with AMPPNP/1Mg *and* peptide (where the O3B is replaced with a nitrogen). Thus, although the nanosecond timescale dynamics of the phosphates are greatly reduced when both MgI and MgII are present, the notable loss of the O3B:MgII interaction in the 2Mg simulations without substrate results in a β-γ-phosphate geometry that is quite different from the TS orientation. Thus, our hypothesis is that the precise β-γ-phosphate coordination and positioning are sensitive to the presence of both the second Mg^{2+} ion (MgI) and the protein substrate. This apparent linkage between β-phosphate positioning and both substrate binding and Mg^{2+}

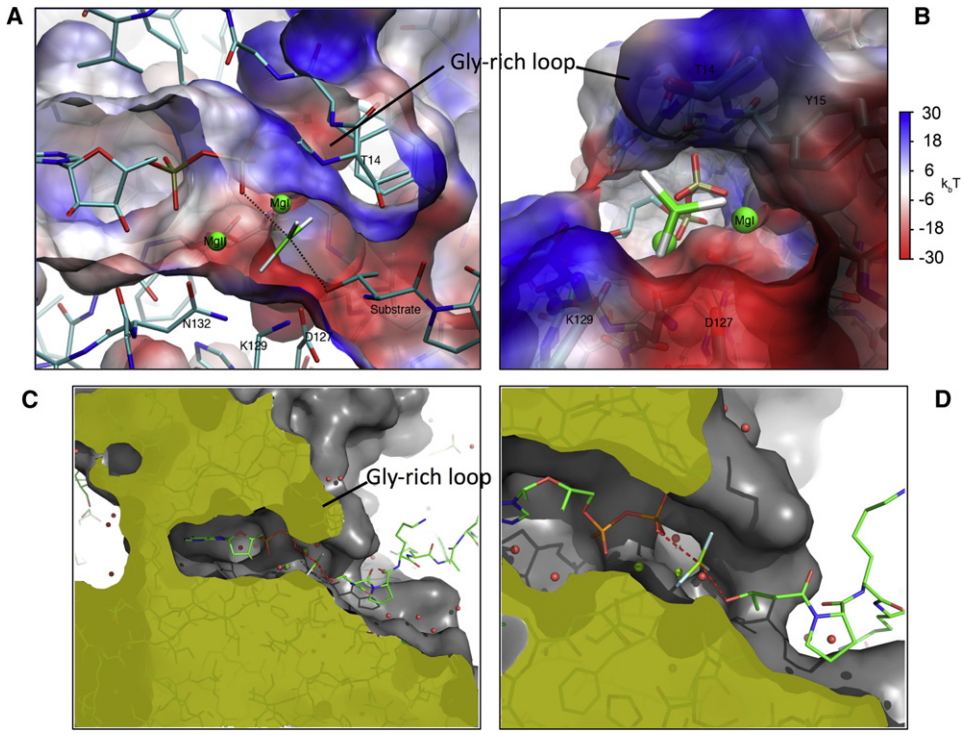

Figure 9. Flexible Glycine Loop

(A and B) Two views of the electrostatic potential in the active site of CDK2 in the TS structure. The scale ranges from −30 kT (red) to 0 kT (white) to +30 kT (blue). Only the protein atoms are included in the calculation, but the ADP (stick), Mg ions (green spheres), and MgF_3^- (stick) are shown for reference. The view in (B) is rotated roughly perpendicular relative to (A) such that the viewpoint is from the perspective of the substrate Thr, along the Thr-MgF_3^--ADP reaction vector. (C and D) Closing of the Gly-rich loop expels solvent and encloses the phosphates. Two slices through a solvent-accessible surface rendering of the active site.

coordination could reduce the probability of a water substituting for the Ser/Thr OH as a nucleophile that would lead to ATP hydrolysis to ADP + P_i, a nonproductive side reaction known to occur for CDK2 and many other activated protein kinases.

DISCUSSION

Roles of the Flexible Glycine-Loop

The flexible Gly-rich loop that rests on top of the nucleotide phosphates is present in most protein kinases and is thus believed to be critical to the function of these enzymes. It is the site of numerous mutations that confer drug resistance to Abl protein kinase (Shah et al., 2002). The protein kinase Gly-rich loop is homologous to the lid-like Gly-rich loop region found in many NTPase enzymes that is often referred to as the P-loop (for phosphate-binding loop, illustrated in Figure S3). This and other similarities support the likelihood that many of the mechanisms used by NTPase enzymes to accelerate the reaction will be related, regardless of the exact details of the catalytic mechanism. For example it has been shown that stabilization of the buildup of negative charge on the β-phosphate of the NDP leaving group can lead to a substantial rate increase for GTPase enzymes (Maegley et al., 1996). This is accomplished in small GTPases by at least three mechanisms, all of which can function as points of regulation: (1) a coordinating Mg^{2+} ion, (2) a cationic side chain such as an Arg "finger" from a GAP, and (3) backbone amide groups from the Gly-rich "P-loop" motif.

We believe that the similar reaction catalyzed by the well-studied small G proteins provides a useful model for understanding aspects of our current CDK2 structure. The presence of a second catalytic Mg^{2+} ion in CDK2 means that CDK2 also utilizes two cations to stabilize the β-phosphate, only replacing the Arg finger with a second Mg^{2+} (Figure S3). The GTPases also help us understand the implications of multiple conformations of the Gly-rich loop in CDK2. One of the most potent oncogenic mutations in small GTPases is a Gly to Val mutation in the Gly-rich P loop that renders the enzymes nearly unable to catalyze the hydrolysis of GTP to GDP, hence, locking them in a perpetual GTP-bound signaling state (Chen et al., 2009; Maegley et al., 1996). This mutation functions by sterically limiting the ability of the P loop amides to adopt the somewhat contorted conformation required to intimately interact with the GTP phosphates and stabilize the buildup of charge during the reaction. Our structure demonstrates how the Gly-rich loop in CDK2 carries out a similar role of electrostatically stabilizing the ATP phosphates during catalysis (Maegley et al., 1996). The positive electrostatic potential presented to the phosphates generated by the down conformation of the Gly-rich loop is depicted in Figures 9A and 9B.

The structural heterogeneity of the CDK2 Gly-rich loop across various structures suggests that the Gly residues fulfill several unique functions: (1) they must be flexible enough to accommodate the closed conformation of the loop; (2) additional flexibility may also be required to allow the Gly-rich loop to open, potentially facilitating nucleotide binding and release; and (3) despite

the lack of functional side chains, the backbone amides of the Gly residues are flexible enough to adopt otherwise unfavorable backbone torsions required to provide optimal electrostatic stabilization of the TS. The protonated Thr14 side chain also contributes to the electrostatic stabilizing potential of the Gly-rich loop. The stabilizing capacity of this residue would be eliminated upon phosphorylation of Thr14 and/or Tyr15 by Myt1/Wee1, two inhibitory modifications of CDK2. Figures 9A and 9B also highlight the strong electronegative coordination environment surrounding both Mg^{2+} sites, testament to the likelihood of localizing divalent ions at both sites.

An additional function of the flexible Gly-rich loop in CDK2 is to exclude solvent surrounding the ATP phosphates. Two views of the tight channel formed around the ATP phosphates in the TS are shown in Figures 9C and 9D. As described above, this closed conformation is stabilized by additional ionic interactions between the phosphates and backbone amides in the Gly-rich loop and only appears to occur once the second Mg^{2+} and substrate peptide have become bound. The substrate/Mg^{2+} activator-triggered closure may function to minimize undesirable ATP hydrolysis that occurs when ATP reacts with a water molecule instead of a substrate Ser/Thr. The exclusion of solvent should also result in an amplification of the electrostatic-stabilizing effects of the Gly-rich loop amides by reducing the dielectric environment surrounding the phosphates.

DFG Motif

The presence of the short Asp-Phe-Gly "DFG" motif is nearly invariant in protein kinases. Located just before the N-terminal end of the activation loop motif (residues 145–147 in CDK2), Asp145 is observed to directly coordinate both of the Mg^{2+} ions at the active site in the TS complex (Figures 5D–5G). The transient occupancy of the MgI ion could have some interesting implications for the functions of this residue. The side chain of Asp145 has been observed to exist in different conformations in some structures of CDK2 bound to nucleotides with 1Mg, such as 1HCK.pdb. Returning again to GTPases as a model, Kannan and Neuwald (2005) pointed out that conformational changes of the homologous Asp residue in GTPases, sometimes induced by the binding of exchange factor proteins (GEFs), can function to destabilize a bound Mg^{2+} ion and facilitate nucleotide exchange. It will be interesting to determine if the observed Asp145 conformational changes play a role in the binding or release of MgI during the catalytic cycle. Wedged in between the two Asp145 oxygens and the ATP β- and γ-phosphates, the MgI site in CDK2 has an extremely negative electrostatic potential, even greater than the nucleotide-free potential shown in Figures 9C and 9D. We have found that when monovalent ions present in our MD simulations spontaneously localize at or near the MgI site, they do not have the same structural, dynamic, or electronic effects as a bound divalent Mg^{2+}. A PROPKA (Bas et al., 2008) calculation of the 1Mg-bound nucleotide state of CDK2 (1QMZ.pdb) suggests that the DFG Asp has a highly elevated pKa (>10.5), and it, or the nucleotide γ-phosphate, may predominantly exist in a protonated state at neutral pH. Because they could shift the equilibrium of MgI binding, both of these observations have important implications for salt and pH effects in the model where the MgI site is only transiently occupied by Mg^{2+}. The DFG-facilitated MgI equilibrium is also consistent with the results of simulations investigating the mechanism of ADP release from PKA that demonstrated that it would be extremely energetically unfavorable to remove the 2Mg-bound ADP from the active site of PKA (Khavrutskii et al., 2009). Like the ordered binding of ATP×1Mg before MgI, the release of MgI may be required to precede the release of ADP.

We believe that this ADP/MgF_3^-/peptide complex represents an informative model for the TS of the phosphoryl-transfer reaction catalyzed by the pCDK2/Cyclin A holoenzyme. This new model proposes that the formation of the catalytically competent active site conformation involves the creation of a transient network of ionic interactions among the protein, the ATP, 2Mg ions, and the substrate peptide. The active site TS conformation is highly homologous to another structure of a protein kinase TS mimic, the ADP/AlF_3/peptide complex of PKA. In order to achieve this active site conformation, the already-activated CDK2 is required to undergo two critical conformational transitions compared with structures lacking any one of the active site ligands: (1) a substantial closing down of the Gly-rich loop, partially stabilized by backbone amide interactions with the β- and γ-phosphates; and (2) a precise ordering of the ATP, particularly the β- and γ-phosphates. More globally, MD simulations suggest that the formation of the TS complex is concurrent with a large-scale dampening of protein and reactant motions in and around the active site. This is partially achieved via the stabilizing effect of replacing nearly every single water-ATP phosphate interaction with direct ionic interactions, particularly interactions with the second catalytic Mg^{2+} and the Gly-rich loop backbone amides, to effectively wedge the N and C-lobes of the kinase together to more tightly engage the dissociating ATP.

Combination of the new crystal structure of the CDK2 kinase described here, with the collection of previous structures and the MD simulations, enables us to construct a more complete model of the dynamic conformational ensemble of CDK2. Before all substrates and two activating Mg^{2+} ions are bound, the active site of the "activated" state of CDK2 is still relatively flexible, and the Gly-rich loop is primarily in an open conformation. The simultaneous occupancy of the ATP, peptide, and 2Mg ion activators increases the ordering of the active site by forming a complex network of ionic interactions where the protein and Mg^{2+} activators engage every one of the ATP phosphate oxygens as well as the substrate side-chain nucleophile. This increased ordering increases the probability of aligning the ATP phosphates in the optimum alignment for catalysis, stabilizes the buildup of negative charge on the phosphate oxygens (destabilizing the β-γ-phosphate linkage), and is correlated with the release of waters from around the phosphates to both enhance the electrostatic field effect of the protein and potentially limit the ATP hydrolysis side reaction.

The inhibition of activity that we observe at high Mg^{2+} concentrations can be rationalized by three models: (1) a second Mg^{2+} slows the rate of ADP product release; (2) ATP bound to 2Mg in solution does not bind as well as ATP×1Mg; and (3) Mg^{2+} has different relative effects on the affinities of ATP and ADP for the protein, resulting in product inhibition. We hope to investigate this phenomenon in more detail in future studies. One conclusion we can make from the observed data is that a single Mg^{2+} ion is not sufficient to achieve maximum reaction velocity.

We believe that the biochemical [Mg^{2+}] data, along with the 2Mg ions identified in the TS crystal structure, are consistent with a model where maximum reaction velocity is achieved when sufficient Mg^{2+} ions are available to bind to both sites, MgI and MgII, but that the occupancy of the MgI site in particular is near equilibrium. It is likely that 2Mg ions are at least transiently necessary to stabilize the phosphoryl-transfer step but that the presence of 2Mg ions may also function to kinetically inhibit other steps in the reaction such as the release of the ADP product. This model accounts for both observations that saturating ATP with 1Mg results in barely observable turnover, whereas even higher concentrations of Mg^{2+} inhibit the reaction. The fact that all previously determined crystal structures of active CDK2 contain a single divalent metal ion had led to much speculation that this kinase only utilizes a single divalent for catalysis. We believe that the current structure and in vitro data suggest that a second divalent ion is utilized at the active site, at least for the phosphoryl-transfer step of the catalytic cycle.

Although it is challenging to measure, there is evidence that intracellular Mg^{2+} ion concentrations vary as a function of the cell cycle (Walker, 1986) and that misregulation of intracellular Mg^{2+} levels may be associated with both cell transformation and increased proliferation (Wolf and Cittadini, 1999). Cell culture studies have identified a correlation between low intracellular Mg^{2+} levels and failure to progress through the G1-S phase transition (Killilea and Ames, 2008), the very checkpoint that is released by CDK2/Cyclin activity. This effect has previously been associated with increased production of the CDK2 inhibitor proteins $P21^{Cip}$ and $P16^{INK}$ (Sgambato et al., 1999) at low [Mg^{2+}]. So, whereas changes in Mg^{2+} ion concentration would most likely have an effect on numerous cellular enzymes, it is possible that the Mg^{2+} dependence of the catalytic subunit of CDK2 enables CDK2 to function as one link between fluctuating local Mg^{2+} concentrations and progression through the cell cycle. ERK2 is anther protein kinase that has been shown to require 2Mg ions and has been proposed to potentially be regulated by physiological fluctuations in intracellular Mg^{2+} levels (Waas and Dalby, 2003).

Our results suggest that the chemistry carried out by CDK2 may indeed be much more similar to PKA than some had expected, whereas at the same time the regulatory mechanisms of these two kinases remain quite different. Data from PKA kinase suggest that the binding of substrates may be coupled to important entropic changes within that protein kinase (Li et al., 2002). It has been determined that still uncharacterized slow conformational transitions may occur at two critical steps of the reaction cycle of PKA: (1) following ATP binding and preceding catalysis, and (2) after catalysis and preceding the release of the reaction products (Shaffer and Adams, 1999a). If we propose that the Gly-rich loop dynamics we observe in CDK2 also takes place in PKA and other kinases, perhaps it is the slow-ordered binding of the second catalytic Mg^{2+} ion and accompanied open to closed transition of the Gly-rich loop that represent the slow conformational change identified to occur after ATP binding to PKA, once hypothesized to represent Mg^{2+} binding (Zhou and Adams, 1997). Similarly, perhaps the subsequent release of the second catalytic Mg represents the second slow conformational transition observed post-catalysis in PKA.

Recent studies of adenylate kinase (ADK) reported that the apo state of that enzyme transiently samples the closed substrate-bound conformation of the enzyme (Henzler-Wildman et al., 2007). It was proposed that the ADK enzyme has been structurally programmed through evolution to sample the TS conformation, and because of this it can more efficiently catalyze the chemical reaction once the substrates do become bound. We believe that CDK2, which is not nearly as efficient an enzyme as ADK (with a roughly 40-fold lower k_{cat}), may have evolved differently. As an integral signaling protein, CDK2 is under evolutionary pressure to be both catalytically efficient as well as robustly regulated. It is a molecular switch. Although it is similar to ADK in that conformational changes are observed upon substrate binding, CDK2 may be different in that it may work to minimize sampling of the TS conformation until it is completely activated. CDK2 appears to maintain relatively high conformational flexibility of the active site and substrates up until the enzyme is fully ready to react, and this precatalytic protein flexibility may function to probabilistically keep the enzyme *away* from sampling the TS conformation until it is the appropriate time to react. Although tolerating this flexibility may have the effect of slowing down the maximum possible rate of the reaction, it may also have evolved to minimize potentially damaging uncontrolled catalytic activity and to facilitate multiple points of regulation of the enzyme. The active site of the fully activated TS complex, including ATP, 2Mg, and peptide substrate, appears to be much more rigid than it is when only ATP and a single Mg^{2+} are bound. Keeping the reactants *rigidly* aligned could represent the most efficient way to increase the probability of a successful nucleophilic attack on the activated γ-phosphate by the activated substrate oxygen, a low-probability event that requires the concerted occurrences of γ-phosphate dissociation and substrate oxygen deprotonation to activate or stabilize the nucleophile. If rigidity is a requirement for the reaction, any number of external influences such as Cyclin binding, Mg activator binding, substrate binding, CDK2 phosphorylation, and assembly of a hydrophobic spine (Kornev et al., 2006) could readily influence catalysis by altering the flexibility of the otherwise flexible and intrinsically inefficient enzyme.

As a final note, we would like to suggest that we believe that each of the growing number of crystal structures of the CDK2 enzyme, when taken together, is providing us a much more complete picture of the different conformations that can be sampled by this flexible enzyme. We are grateful that so many different structures of this single enzyme have been made available in the protein databank (Berman et al., 2002).

EXPERIMENTAL PROCEDURES

Detailed methods are included in the Supplemental Experimental Procedures.

The pCDK2/Cyclin A complex was generated by coexpression of three vectors containing CDK2, Cyclin A, and Cak1p in *E. coli*. Crystals were generated by growing crystals of the apo pCDK2/Cyclin A complex using vapor diffusion with 22% w/v Poly(acrylic acid sodium salt) 5, 100, and 20 mM $MgCl_2$, 100 mM HEPES, and then soaking these crystals with the active site ligands prior to cryoprotection. X-ray diffraction data were collected at LS-CAT (APS). Initial models were generated with molecular replacement, and refinement was carried out using PHENIX. Enzyme kinetics were carried out using either a coupled kinase reaction with Histone H1 substrate or a P^{32}-labeled

ATP assay using peptide substrate. All MD simulations were carried out using the AMBER 10.0 package (Pearlman et al., 1995) and FF99SB force field (Hornak et al., 2006).

ACCESSION NUMBERS

Atomic coordinates and structure factors have been deposited in the RCSB Protein Data Bank with accession codes 3QHR and 3QHW.

SUPPLEMENTAL INFORMATION

Supplemental Information includes Supplemental Experimental Procedures and three figures and can be found with this article online at doi:10.1016/j.str.2011.02.016.

ACKNOWLEDGMENTS

D.M.J. was supported by Bioinformatics Training Program T32 GM070449-05 and Proteome Informatics of Cancer Training Program T32 CA140044-01. M.A.Y. was supported by Burroughs Wellcome career award at the scientific interface 1003999. We thank Bernard Rupp for advice during refinement and Peng Jiang for assistance with ATP P32 assays. We thank all of the support staff at the APS LS-CAT beamlines.

Received: July 27, 2010
Revised: January 26, 2011
Accepted: February 7, 2011
Published: May 10, 2011

REFERENCES

Adams, J.A. (2001). Kinetic and catalytic mechanisms of protein kinases. Chem. Rev. *101*, 2271–2290.

Adams, P.D., Afonine, P.V., Bunkóczi, G., Chen, V.B., Davis, I.W., Echols, N., Headd, J.J., Hung, L.W., Kapral, G.J., Grosse-Kunstleve, R.W., et al. (2010). PHENIX: a comprehensive Python-based system for macromolecular structure solution. Acta Crystallogr. D Biol. Crystallogr. *66*, 213–221.

Bas, D.C., Rogers, D.M., and Jensen, J.H. (2008). Very fast prediction and rationalization of pKa values for protein-ligand complexes. Proteins *73*, 765–783.

Baxter, N.J., Olguin, L.F., Golicnik, M., Feng, G., Hounslow, A.M., Bermel, W., Blackburn, G.M., Hollfelder, F., Waltho, J.P., and Williams, N.H. (2006). A Trojan horse transition state analogue generated by MgF3− formation in an enzyme active site. Proc. Natl. Acad. Sci. USA *103*, 14732–14737.

Baxter, N.J., Blackburn, G.M., Marston, J.P., Hounslow, A.M., Cliff, M.J., Bermel, W., Williams, N.H., Hollfelder, F., Wemmer, D.E., and Waltho, J.P. (2008). Anionic charge is prioritized over geometry in aluminum and magnesium fluoride transition state analogs of phosphoryl transfer enzymes. J. Am. Chem. Soc. *130*, 3952–3958.

Berman, H.M., Battistuz, T., Bhat, T.N., Bluhm, W.F., Bourne, P.E., Burkhardt, K., Feng, Z., Gilliland, G.L., Iype, L., Jain, S., et al. (2002). The Protein Data Bank. Acta Crystallogr. D Biol. Crystallogr. *58*, 899–907.

Brown, N.R., Noble, M.E., Endicott, J.A., and Johnson, L.N. (1999a). The structural basis for specificity of substrate and recruitment peptides for cyclin-dependent kinases. Nat. Cell Biol. *1*, 438–443.

Brown, N.R., Noble, M.E., Lawrie, A.M., Morris, M.C., Tunnah, P., Divita, G., Johnson, L.N., and Endicott, J.A. (1999b). Effects of phosphorylation of threonine 160 on cyclin-dependent kinase 2 structure and activity. J. Biol. Chem. *274*, 8746–8756.

Chen, X., Mitsutake, N., LaPerle, K., Akeno, N., Zanzonico, P., Longo, V.A., Mitsutake, S., Kimura, E.T., Geiger, H., Santos, E., et al. (2009). Endogenous expression of Hras(G12V) induces developmental defects and neoplasms with copy number imbalances of the oncogene. Proc. Natl. Acad. Sci. USA *106*, 7979–7984.

Cook, P.F., Neville, M.E., Jr., Vrana, K.E., Hartl, F.T., and Roskoski, R., Jr. (1982). Adenosine cyclic 3′,5′-monophosphate dependent protein kinase: kinetic mechanism for the bovine skeletal muscle catalytic subunit. Biochemistry *21*, 5794–5799.

Cook, A., Lowe, E.D., Chrysina, E.D., Skamnaki, V.T., Oikonomakos, N.G., and Johnson, L.N. (2002). Structural studies on phospho-CDK2/cyclin A bound to nitrate, a transition state analogue: implications for the protein kinase mechanism. Biochemistry *41*, 7301–7311.

DeLano, W. (2010). The PyMOL Molecular Graphics System. Version 1.3, Schrödinger, LLC, http://www.pymol.org/citing.

De Vivo, M., Cavalli, A., Carloni, P., and Recanatini, M. (2007). Computational study of the phosphoryl transfer catalyzed by a cyclin-dependent kinase. Chemistry *13*, 8437–8444.

Dudev, T., and Lim, C. (2004). Monodentate versus bidentate carboxylate binding in magnesium and calcium proteins: what are the basic principles? J. Phys. Chem. B *108*, 4546–4557.

Graham, D.L., Lowe, P.N., Grime, G.W., Marsh, M., Rittinger, K., Smerdon, S.J., Gamblin, S.J., and Eccleston, J.F. (2002). MgF(3)(-) as a transition state analog of phosphoryl transfer. Chem. Biol. *9*, 375–381.

Greenman, C., Stephens, P., Smith, R., Dalgliesh, G.L., Hunter, C., Bignell, G., Davies, H., Teague, J., Butler, A., Stevens, C., et al. (2007). Patterns of somatic mutation in human cancer genomes. Nature *446*, 153–158.

Henzler-Wildman, K.A., Thai, V., Lei, M., Ott, M., Wolf-Watz, M., Fenn, T., Pozharski, E., Wilson, M.A., Petsko, G.A., Karplus, M., et al. (2007). Intrinsic motions along an enzymatic reaction trajectory. Nature *450*, 838–844.

Hornak, V., Abel, R., Okur, A., Strockbine, B., Roitberg, A., and Simmerling, C. (2006). Comparison of multiple amber force fields and development of improved protein backbone parameters. Proteins *65*, 712–725.

Huse, M., and Kuriyan, J. (2002). The conformational plasticity of protein kinases. Cell *109*, 275–282.

Jeffrey, P.D., Russo, A.A., Polyak, K., Gibbs, E., Hurwitz, J., Massague, J., and Pavletich, N.P. (1995). Mechanism of CDK activation revealed by the structure of a cyclinA-CDK2 complex. Nature *376*, 313–320.

Kamerlin, S.C., and Warshel, A. (2010). At the dawn of the 21st century: is dynamics the missing link for understanding enzyme catalysis? Proteins *78*, 1339–1375.

Kannan, N., and Neuwald, A.F. (2005). Did protein kinase regulatory mechanisms evolve through elaboration of a simple structural component? J. Mol. Biol. *351*, 956–972.

Khavrutskii, I.V., Grant, B., Taylor, S.S., and McCammon, J.A. (2009). A transition path ensemble study reveals a linchpin role for Mg(2+) during rate-limiting ADP release from protein kinase A. Biochemistry *48*, 11532–11545.

Killilea, D.W., and Ames, B.N. (2008). Magnesium deficiency accelerates cellular senescence in cultured human fibroblasts. Proc. Natl. Acad. Sci. USA *105*, 5768–5773.

Kornev, A.P., Haste, N.M., Taylor, S.S., and Eyck, L.F. (2006). Surface comparison of active and inactive protein kinases identifies a conserved activation mechanism. Proc. Natl. Acad. Sci. USA *103*, 17783–17788.

Li, F., Gangal, M., Juliano, C., Gorfain, E., Taylor, S.S., and Johnson, D.A. (2002). Evidence for an internal entropy contribution to phosphoryl transfer: a study of domain closure, backbone flexibility, and the catalytic cycle of cAMP-dependent protein kinase. J. Mol. Biol. *315*, 459–469.

Liu, Y., and Gray, N.S. (2006). Rational design of inhibitors that bind to inactive kinase conformations. Nat. Chem. Biol. *2*, 358–364.

Liu, M., Girma, E., Glicksman, M.A., and Stein, R.L. (2010). Kinetic mechanistic studies of Cdk5/p25-catalyzed H1P phosphorylation: metal effect and solvent kinetic isotope effect. Biochemistry *49*, 4921–4929.

Madhusudan, Akamine, P., Xuong, N.H., and Taylor, S.S. (2002). Crystal structure of a transition state mimic of the catalytic subunit of cAMP-dependent protein kinase. Nat. Struct. Biol. *9*, 273–277.

Maegley, K.A., Admiraal, S.J., and Herschlag, D. (1996). Ras-catalyzed hydrolysis of GTP: a new perspective from model studies. Proc. Natl. Acad. Sci. USA *93*, 8160–8166.

Malumbres, M., and Barbacid, M. (2007). Cell cycle kinases in cancer. Curr. Opin. Genet. Dev. *17*, 60–65.

Malumbres, M., and Barbacid, M. (2009). Cell cycle, CDKs and cancer: a changing paradigm. Nat. Rev. Cancer *9*, 153–166.

Manning, G., Whyte, D.B., Martinez, R., Hunter, T., and Sudarsanam, S. (2002). The protein kinase complement of the human genome. Science *298*, 1912–1934.

Masterson, L.R., Cheng, C., Yu, T., Tonelli, M., Kornev, A., Taylor, S.S., and Veglia, G. (2010). Dynamics connect substrate recognition to catalysis in protein kinase A. Nat. Chem. Biol. *6*, 821–828.

Milde-Langosch, K., Bamberger, A.M., Goemann, C., Rossing, E., Rieck, G., Kelp, B., and Loning, T. (2001). Expression of cell-cycle regulatory proteins in endometrial carcinomas: correlations with hormone receptor status and clinicopathologic parameters. J. Cancer Res. Clin. Oncol. *127*, 537–544.

Mildvan, A.S. (1997). Mechanisms of signaling and related enzymes. Proteins *29*, 401–416.

Morgan, D.O. (1997). Cyclin-dependent kinases: engines, clocks, and microprocessors. Annu. Rev. Cell Dev. Biol. *13*, 261–291.

Mukherjee, K., Sharma, M., Urlaub, H., Bourenkov, G.P., Jahn, R., Südhof, T.C., and Wahl, M.C. (2008). CASK functions as a Mg2+-independent neurexin kinase. Cell *133*, 328–339.

O'Sullivan, W.J., and Smithers, G.W. (1979). Stability constants for biologically important metal-ligand complexes. Methods Enzymol. *63*, 294–336.

Pavletich, N.P. (1999). Mechanisms of cyclin-dependent kinase regulation: structures of Cdks, their cyclin activators, and Cip and INK4 inhibitors. J. Mol. Biol. *287*, 821–828.

Pearlman, D.A., Case, D.A., Caldwell, J.W., Ross, W.S., Cheatham, T.E., III, DeBolt, S., Ferguson, D., Seibel, G., and Kollman, P. (1995). AMBER, a package of computer programs for applying molecular mechanics, normal mode analysis, molecular dynamics and free energy calculations to simulate the structural and energetic properties of molecules. Comput. Phys. Commmun. *91*, 1–41.

Radzio-Andzelm, E., Lew, J., and Taylor, S. (1995). Bound to activate: conformational consequences of cyclin binding to CDK2. Structure *3*, 1135–1141.

Russo, A.A., Jeffrey, P.D., and Pavletich, N.P. (1996). Structural basis of cyclin-dependent kinase activation by phosphorylation. Nat. Struct. Biol. *3*, 696–700.

Schulze-Gahmen, U., De Bondt, H.L., and Kim, S.H. (1996). High-resolution crystal structures of human cyclin-dependent kinase 2 with and without ATP: bound waters and natural ligand as guides for inhibitor design. J. Med. Chem. *39*, 4540–4546.

Sgambato, A., Wolf, F.I., Faraglia, B., and Cittadini, A. (1999). Magnesium depletion causes growth inhibition, reduced expression of cyclin D1, and increased expression of P27Kip1 in normal but not in transformed mammary epithelial cells. J. Cell. Physiol. *180*, 245–254.

Shaffer, J., and Adams, J.A. (1999a). An ATP-linked structural change in protein kinase A precedes phosphoryl transfer under physiological magnesium concentrations. Biochemistry *38*, 5572–5581.

Shaffer, J., and Adams, J.A. (1999b). Detection of conformational changes along the kinetic pathway of protein kinase A using a catalytic trapping technique. Biochemistry *38*, 12072–12079.

Shah, N.P., Nicoll, J.M., Nagar, B., Gorre, M.E., Paquette, R.L., Kuriyan, J., and Sawyers, C.L. (2002). Multiple BCR-ABL kinase domain mutations confer polyclonal resistance to the tyrosine kinase inhibitor imatinib (STI571) in chronic phase and blast crisis chronic myeloid leukemia. Cancer Cell *2*, 117–125.

Stevenson, L.M., Deal, M.S., Hagopian, J.C., and Lew, J. (2002). Activation mechanism of CDK2: role of cyclin binding versus phosphorylation. Biochemistry *41*, 8528–8534.

Sun, G., and Budde, R.J. (1997). Requirement for an additional divalent metal cation to activate protein tyrosine kinases. Biochemistry *36*, 2139–2146.

Valiev, M., Kawai, R., Adams, J.A., and Weare, J.H. (2003). The role of the putative catalytic base in the phosphoryl transfer reaction in a protein kinase: first-principles calculations. J. Am. Chem. Soc. *125*, 9926–9927.

Waas, W.F., and Dalby, K.N. (2003). Physiological concentrations of divalent magnesium ion activate the serine/threonine specific protein kinase ERK2. Biochemistry *42*, 2960–2970.

Walker, G.M. (1986). Magnesium and cell cycle control: an update. Magnesium *5*, 9–23.

Westheimer, F.H. (1987). Why nature chose phosphates. Science *235*, 1173–1178.

Wolf, F.I., and Cittadini, A. (1999). Magnesium in cell proliferation and differentiation. Front Biosci. *4*, D607–D617.

Zhou, J., and Adams, J.A. (1997). Is there a catalytic base in the active site of cAMP-dependent protein kinase? Biochemistry *36*, 2977–2984.

Zimmermann, B., Schweinsberg, S., Drewianka, S., and Herberg, F.W. (2008). Effect of metal ions on high-affinity binding of pseudosubstrate inhibitors to PKA. Biochem. J. *413*, 93–101.

